Radiotherapy and Oncology xxx (xxxx) xxx

Contents lists available at ScienceDirect

Radiotherapy and Oncology

journal homepage: www.thegreenjournal.com

Original Article

Trade-off in healthy tissue sparing of FLASH and fractionation in stereotactic proton therapy of lung lesions with transmission beams

Steven Habraken [a,b,*,1], Sebastiaan Breedveld [a], Jort Groen [a,2], Joost Nuyttens [a,c], Mischa Hoogeman [a,b]

[a] Erasmus MC Cancer Institute, University Medical Center Rotterdam, Department of Radiotherapy, Rotterdam, The Netherlands; [b] Holland Proton Therapy Center, Department of Medical Physics & Informatics; and [c] Holland Proton Therapy Center, Department Radiation Oncology, Delft, The Netherlands

ARTICLE INFO

Article history:
Received 25 February 2022
Received in revised form 12 August 2022
Accepted 14 August 2022
Available online xxxx

Keywords:
Stereotactic lung treatment
Proton therapy
Flash radiotherapy
Radiobiological modeling
Treatment planning

ABSTRACT

Purpose and objective: Besides a dose-rate threshold of 40–100 Gy/s, the FLASH effect may require a dose > 3.5–7 Gy. Even in hypofractioned treatments, with all beams delivered in each fraction (ABEF), most healthy tissue is irradiated to a lower fraction dose. This can be circumvented by single-beam-per-fraction (SBPF) delivery, with a loss of healthy tissue sparing by fractionation. We investigated the trade-off between FLASH and loss of fractionation in SBPF stereotactic proton therapy of lung cancer and determined break-even FLASH-enhancement ratios (FERs).

Materials and Methods: Treatment plans for 12 patients were generated. GTV delineations were available and a 5 mm GTV-PTV margin was applied. Equiangular arrangements of 3, 5, 7, and 9 244 MeV proton transmission beams were used. To facilitate SBPF, the number of fractions was equal to the number of beams. Iso-effective fractionation schedules with a single field uniform dose prescription were used: $D_{95\%,PTV}$ = 100%D_{pres} per beam. All plans were evaluated in terms of dose to lung and conformity of dose to target of FLASH-enhanced biologically equivalent dose (EQD2).

Results: Compared to ABEF, SBPF resulted in a median increase of $EQD2_{mean}$ to healthy lung of 56%, 58%, 55% and 54% in plans with 3, 5, 7 and 9 fractions respectively and of 236%, 78%, 50% and 41% in $V_{100\%\ EQD2}$, quantifying conformity. This can be compensated for by FERs of at least 1.28, 1.32, 1.30 and 1.23 respectively for $EQD2_{mean}$ and 1.29, 1.18, 1.28 and 1.15 for $V_{100\%,EQD2}$.

Conclusion: A FLASH effect outweighing the loss of fractionation in SBPF may be achieved in stereotactic lung treatments. The trade-off with fractionation depends on the conditions under which the FLASH effect occurs. Better understanding of the underlying biology and the impact of delivery conditions is needed.

Since its discovery in 2014 [1], FLASH as a differential effect between tumors and healthy tissue has attracted a lot attention in radiotherapy [2–4]. It has been consistently observed in radiobiological experiments in animals and amounts to a reduction of the radiosensitivity of healthy tissue in ultra-high dose rate (>40–100 Gy/s) high dose (>3.5–7 Gy) [4] irradiation, relative to that of the tumor. While the dependence of radiosensitivity on dose rate and oxygenation has been known since the 1960s [5], FLASH as a differential effect provides a novel and fundamentally different way to further increase the therapeutic bandwidth of radiotherapy - in addition to fractionation and high-precision irradiation techniques with image guidance.

Most animal experiments have been performed with high-dose rate electron beams, focusing e.g., on neurocognitive function [6], lung fibrosis [1], skin [7] and abdominal toxicities [8] as healthy tissue end points. FLASH has also been demonstrated in a first patient treatment [9]. Ultra-high dose rates are readily available in cyclotron-accelerated therapeutic proton beams [10] and evidence is gathering that the FLASH effect exists in such beams [11–15]. FLASH proton therapy (FLASH-PT) holds the promise of combining the FLASH effect with the physical advantages of proton beams. It is particularly well-suited for deep-seated targets. Recently, accrual for a first clinical trials on FLASH-PT with pencil beam scanning (PBS) has been completed [16].

* Corresponding author at: Erasmus University Medical Center, Department of Radiotherapy – Medical Physics and Instrumentation, Postbus 2040, 3000 CA Rotterdam, The Netherlands.
E-mail address: s.habraken@erasmusmc.nl (S. Habraken).
[1] Visiting address: Erasmus University Medical Center, Department of Radiotherapy – Medical Physics and Instrumentation, Dr. Molewaterplein 40, 3015 GD Rotterdam, The Netherlands.
[2] Current affiliation: Amsterdam University Medical Center, Department of Radiation Oncology, Amsterdam, The Netherlands.

https://doi.org/10.1016/j.radonc.2022.08.015
0167-8140/

With protons, the overall highest dose rate is achieved at the maximum cyclotron energy of 250 MeV. Such beams have a 38 cm range in water and shoot through the patient in the first foreseen clinical applications, e.g. bone metastases and thoracic lesions [17–20]. Their use may come at the expense of conformity of dose to the target. Moreover, as the FLASH effect comes with a fraction dose threshold of 3.5–7 Gy [4], clinically, it is limited to hypofractionated treatments.

With delivery of all beams in each fraction (ABEF) of, e.g., 54 Gy with 3 beams in 3 fractions, the beam doses of 6 Gy may fall below the FLASH threshold, compromising FLASH in healthy tissue irradiated by one beam only. In the volume with overlapping beams from different angles, the average dose rate is compromised by gantry and couch shifting times to values far below the FLASH dose-rate threshold of 40–100 Gy/s. It is not clear yet to what extend the FLASH effect exists in revisits of the same OAR voxels in one fraction. This can be circumvented by single beam per fraction (SBPF) delivery with single-field uniform dose (SFUD) treatment planning to ensure adequate target dose in each fraction. SFUD, however, limits conformity of physical dose, and SBPF comes with a loss of healthy tissue sparing by fractionation, further compromising conformity of biologically equivalent dose.

To assess (i) the clinical feasibility of stereotactic FLASH-PT in clinically realistic hypofractionated treatments and (ii) which biological aspects/unknowns are important for clinical translatability, we investigated the trade-off between the FLASH effect and loss of fractionation in FLASH-enhanced SBPF vs ABEF delivery of the same treatment plans in stereotactic proton therapy of small lung lesions. As 18 Gy per fraction with a single beam may not be clinically acceptable in all patients, we focused on different isoeffective fractionation regimens derived from 54 Gy in 3 fractions and α/β = 10 Gy for the target. Lung function can be critical in these patients, both in case of primary lung cancer and in a metastatic setting. Therefore, we evaluated dose to healthy lung and the volume receiving 100% of prescribed biologically equivalent dose for different FLASH enhancement ratios (FERs). Since the equivalent dose to healthy lung is increased by SBPF delivery, we also calculated break-even FERs for which SFBF is on par with ABEF delivery of the same plans.

Method and materials

Patient data

Anonymized planning-CT scans and delineations of 12 patients with primary lung cancer and lung metastasis, clinically treated with photons in prone (5) or supine (7) position, were used. GTV delineations were available and an isotropic 5 mm GTV-PTV margin was applied. Only small PTVs (median 6.4 cc, range 4.4–10.1 cc) and only one lesion per patient, 3 right-sided and 12 left-sided, were included. The median GTV volume was 1.2 cc (range 0.5–2.6 cc).

Treatment planning

Treatment plans with 244 MeV proton transmission (shoot-through) beams, the highest energy currently commissioned, was implemented in Erasmus-iCycle, our in-house developed software for automated prioritized optimization of radiotherapy treatment plans [21], using the HollandPTC clinical proton beam model and the Astroid dose engine [22,23].

For this study the common fractionation schedule of 54 Gy in 3 fractions [24] was used. To evaluate the impact of fractionation with more moderate yet FLASH-compatible fraction doses, we also considered 65.5 Gy in 5, 73.7 Gy in 7 and 80.0 Gy in 9 fractions, see supplementary material [SM]. These are isoeffective fractionation regimens based on 54 Gy in 3 fractions[3] assuming a radiobiological α/β ratio of 10 Gy for the target. The number of beams was kept equal to the number of treatment fractions, to facilitate FLASH-enhanced SBPF delivery, allowing for a direct comparison to delivery of all beams in each fraction (ABEF).

Table 1
Constraints and objectives in treatment planning.

Target/OAR	Constraint	Objectives
CVT = GTV	$D_{min} \geq D_{pres}$	$D_{max} \leq 124\%\ D_{pres}$
PTV minus GTV	$D_{min} = 98\%\ D_{pres}$	$D_{max} \leq 124\%\ D_{pres}$ $D_{3mm\ shell} \leq 62\%\ D_{pres}$ $D_{6mm\ shell} \leq 31\%\ D_{pres}$ $D_{9\ mm\ shell} = 0$ Gy $D_{20\ mm\ shell} = 0$ Gy
Ipsilateral lung minus PTV + 20 mm	$D_{max} \leq 32\%\ D_{pres}$	$D_{max} = 0$ Gy $D_{mean} = 0$ Gy
Contralateral lung	$D_{max} \leq 32\%\ D_{pres}$	$D_{max} = 0$ Gy $D_{mean} = 0$ Gy
Esophagus	$D_{max} \leq 31.5$ Gy	$D_{max} \leq 24$ Gy
Spinal cord	$D_{max} \leq 21.6$ Gy	$D_{max} \leq 18$ Gy
Trachea	$D_{max} \leq 36$ Gy	$D_{max} \leq 33$ Gy
Ipsilateral bronchus	$D_{max} \leq 38.1$ Gy	$D_{max} \leq 36$ Gy
Liver, stomach, bowel	Avoid	

An SFUD approach with transmission beams was used with: $D_{95\%,PTV} = 100\%\ D_{pres}$ per beam. Dosimetric constraints were put on (i) minimum dose to GTV and PTV (ii) maximum dose to critical serial OARs and (iii) dose to contralateral lung and to ipsilateral lung minus a 20 mm expansion of the PTV. Prioritized objectives were used on (i) maximum dose to PTV, (ii) maximum dose to GTV, (iii) 3 mm and 6 mm shells around the PTV and (iv) dose to all OARs and other non-specified tissue, see also Table 1. The initial set of pencil beams was chosen on a 5 mm lateral grid. Pencil-beam selection [25] was used to reduce the number of transmission pencil beams and, hence, delivery time. Co-planar equiangular arrangements of beams were used to mimize beam overlap and improve conformity of dose to the target. The overall orientation was chosen so as to maximally avoid serial OARs, i.e., esophagus and spinal cord.

FLASH and fractionation modeling

Treatment delivery and fractionation regimens were evaluated in terms of the total equivalent dose in 2 Gy fractions (EQD2), defined as $EQD2(d,D) = (\alpha/\beta + d)D/(\alpha/\beta + 2\ Gy)$, with the fraction dose d, the total dose $D = n \times d$, n the number of fractions and α/β the ratio of radiobiological α and β parameters. We assumed α/β = 3 Gy for all healthy tissues. Since FLASH is a fraction dose effect [4], the FLASH enhancement ratio (FER, ≥ 1) was applied to all physical fraction voxel doses, i.e., $d_j \rightarrow d_j$ /FER to all OAR voxels j, with no threshold within a beam.

Evaluation

FLASH-enhanced EQD2 distributions for ABEF and SBPF delivery were calculated for FERs from 1.0 (no FLASH effect) to 2.0 in steps of 0.05. Voxel fraction EQD2s for FLASH-enhanced single-beam per fraction delivery were summed up for all fractions. The total EQD2 distributions were evaluated in terms of mean dose to ipsilateral lung ($EQD2_{mean}$). As both SFUD planning with transmission beams and SBPF delivery come at the expense of conformity of EQD2 to

[3] Since proton dose in the entrance part of the beam is low-LET irradiation, no RBE-weighting was used.

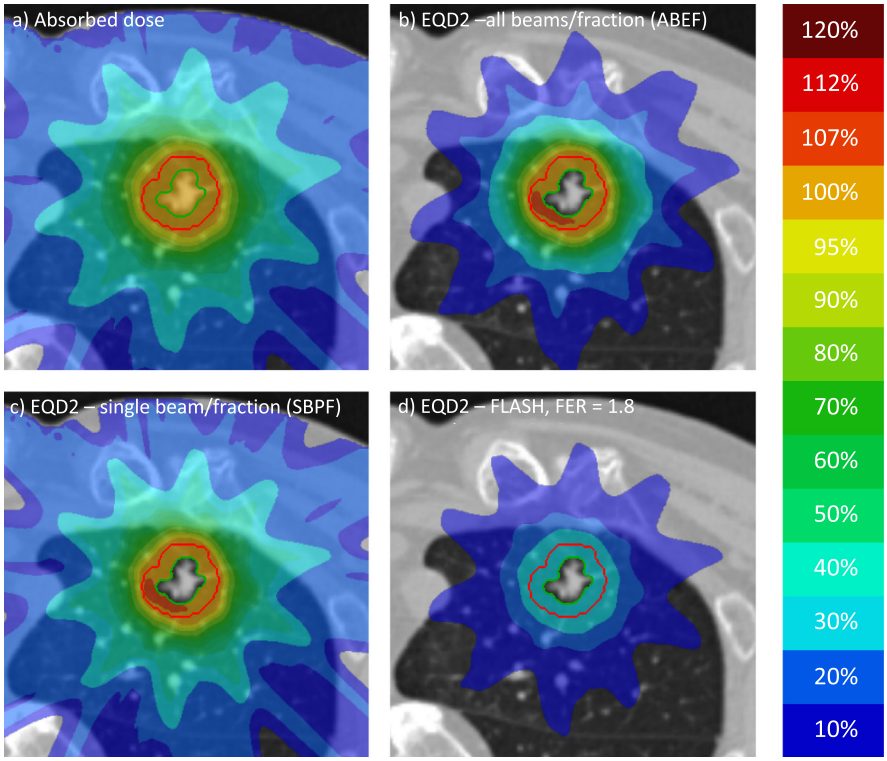

Fig. 1. (a) Absorbed dose distribution for a treatment plan with five equiangular 244 MeV transmission beams. Depending on delivery and the FLASH effect, this leads to the EQD2 distributions in panel (b)-(d). Panel (b) shows the EQD2 distribution for conventional delivery of all beams in each fraction (ABEF), while panel (c) shows that of non-FLASH-enhanced single-beam per fraction (SBPF) delivery. The difference between (b) and (c) shows the effect of the loss of fractionation. Panel (d) shows the EQD2 distribution for FLASH-enhanced SPBF delivery with FER = 1.8. At this FER, the FLASH effect more than compensates the loss of healthy tissue sparing through fractionation. The EQD2 is calculated in healthy tissue outside the GTV only, with $\alpha/\beta = 3$ Gy. From blue to red, the isofill levels correspond to 10% – 120% of 65.5 Gy for the absorbed dose in panel (a) and the corresponding EQD2 of 210.9 Gy in panels (b)-(d) respectively. The GTV and PTV contours are displayed in green and red respectively.

the target, also the volume receiving 100% of the prescribed dose ($V_{100\%\ EQD2pres}$) was evaluated. Since the target is included, for maximum OAR sparing this is equal to the GTV. To evaluate the $V_{100\%\ EQD2pres}$, prescribed doses of 54 Gy in 3, 65.5 Gy in 5, 73.7 Gy in 7 and 80.0 Gy in 9 fractions were converted to EQD2 with $\alpha/\beta = 3$ Gy, i.e., 226.8 Gy, 210.9 Gy, 199.4 Gy and 190.2 Gy for 3, 5, 7 and 9 fraction plans respectively. FLASH-enhanced values of $EQD2_{mean}$ and $V_{100\%\ EQD2pres}$ were normalized to non-FLASH-enhanced values for the ABEF results for each patient, and population median and full ranges (minimum to maximum) were calculated. Break-even FERs, i.e., the FER at which the FLASH effect compensates for the loss of healthy tissue sparing through fractionation in SBPF delivery, were calculated by linear interpolation between the data points. Linear interpolation of the data points to FER intervals of 0.01 was used to calculate cumulative population break-even histograms. These quantify the fraction of patients benefiting from FLASH as a function of FER.

Delivery times

Treatment planning was based on integral dose-depth profiles, normalized to D_{max} in water. Delivery times were calculated based on 0.3 Gprotons per unit beam weight,[4] a proton beam current of 220nA at the nozzle and a switching time of 0.2 ms between pencil beams. Beam dose rates are calculated as the nominal dose per beam, divided by the delivery time.

[4] Integral dose-depth (IDD) curves, normalized to D_{max} are used in Erasmus-iCycle. For typical beam parameters, the dose to D_{max} for 244 MeV protons is estimated from an analytical dose model as 3 Gy/Gproton [24].

Results

All target planning constraints were met in all treatment plans. A typical example of the total absorbed dose, the EQD2 for conventional ABEF delivery, SBPF without FLASH enhancement and SBPF delivery with a FER of 1.8 are shown in Fig. 1. Also, all OAR constraints were met in all treatment plans. Non-FLASH-enhanced values for the $EQD2_{mean}$ to healthy ipsilateral lung and the $V_{100\%\ EQD2pres}$ for ABEF and SBPF delivery are shown in Fig. 2. The loss of fractionation is substantial, leading to a median increase of $EQD2_{mean}$ to healthy lung of 56%, 58%, 55% and 54% in plans with 3, 5, 7 and 9 fractions respectively and a median increase of 236%, 78%, 50% and 41% in $V_{100\%\ EQD2}$. Patient population ranges of these percentage losses are listed in Table 2. As can also be seen in Fig. 2, a median reduction of 54% (full range: 44%-69%) of the $V_{100\%\ EQD2pres}$ in SBPF delivery can be achieved by using 5 instead of 3 beams. Median reductions of 67% (55%-79%) and 73% (65%-82%) can be achieved with 7 and 9 beams respectively (relative to 3 beams).

The dependence on FER of $EQD2_{mean}$ and the $V_{100\%\ EQD2pres}$ for all patients and plans is shown in the panels of Fig. 3. The graphs display patient population median values while the error bars indicate the full population range, i.e., the overall minimum and maximum values. Break-even FERs for $EQD2_{mean}$ and $V_{100\%\ EQD2pres}$, i.e., the values of the FER at which the fractionation disadvantage is outweighed by the FLASH effect, are listed in Table 2, where, for reference, also the $EQD2_{mean}$ and $V_{100\%\ EQD2pres}$ obtained for ABEF delivery are listed. The break-even FER for the $EQD2_{mean}$ lies around 1.3 and hardly depends on the number of beams and fractions. Break-even FERs for the $V_{100\%\ EQD2pres}$

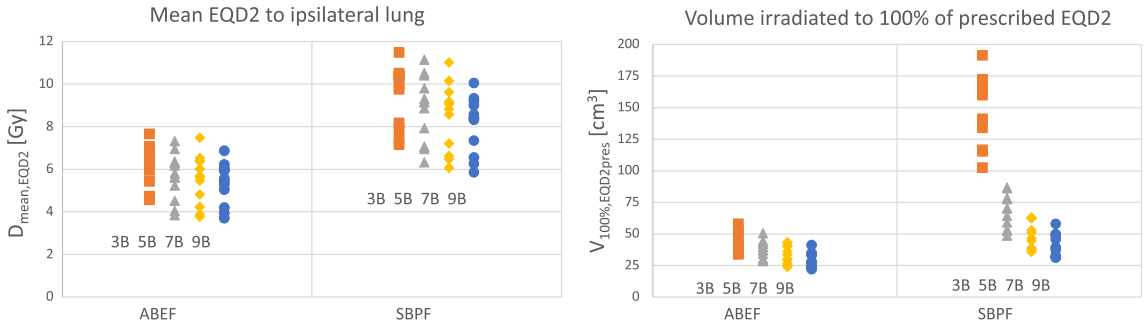

Fig. 2. $EQD2_{mean}$ to ipsilateral lung and $V_{100\%\ EQD2pres}$ for all patients and different non-FLASH enhanced treatment delivery techniques. On the left, results are shown for all beam in each fraction delivery of SFUD plans with 244 MeV transmission beams (ABEF) while results for non-FLASH enhanced single-beam per fraction of the SFUD plans (SBPF) are shown on the right. Results for plans with 3, 5, 7 and 9 beams/fractions are displayed in orange, gray, yellow, and blue respectively. Each data point corresponds to one patient.

Table 2
Reference values of $EQD2_{mean}$ and $V_{100\%\ EQD2pres}$ in ABEF delivery, percentage increase of the $EQD2_{mean}$ and $V_{100\%\ EQD2pres}$ in SBPF delivery, relative to ABEF delivery and break-even (BE) FERs for $EQD2_{mean}$ and $V_{100\%\ EQD2pres}$ for which the FLASH effect compensates for the loss of fractionation.

	$EQD2_{mean}$ [Gy]	$V_{100\%\ EQD2pres}$ [cc]	SBPF/ABEF $EQD2_{mean}$	SBPF/ABEF $V_{100\%\ EQD2pres}$	BE-$EQD2_{mean,\ lung\ -\ GTV}$	BE-$V_{100\%\ EQD2pres}$
3B	6.4 (4.6–7.6)	42 (34–58)	56% (46–69%)	236% (166%-380%)	1.278 (1.233–1.339)	1.325 (1.300–1.360)
5B	5.7 (3.8–7.3)	37 (28–51)	58% (44%-74%)	78% (61%-95%)	1.298 (1.231–1.376)	1.230 (1.225–1.240)
7B	5.6 (3.8–7.5)	32 (24–43)	55% (39%-71%)	50% (44%-58%)	1.291 (1.211–1.369)	1.175 (1.150–1.200)
9B	5.5 (3.7–6.9)	27 (22–41)	54% (40%-66%)	41% (30%-48%)	1.282 (1.218–1.355)	1.150 (1.100–1.150)

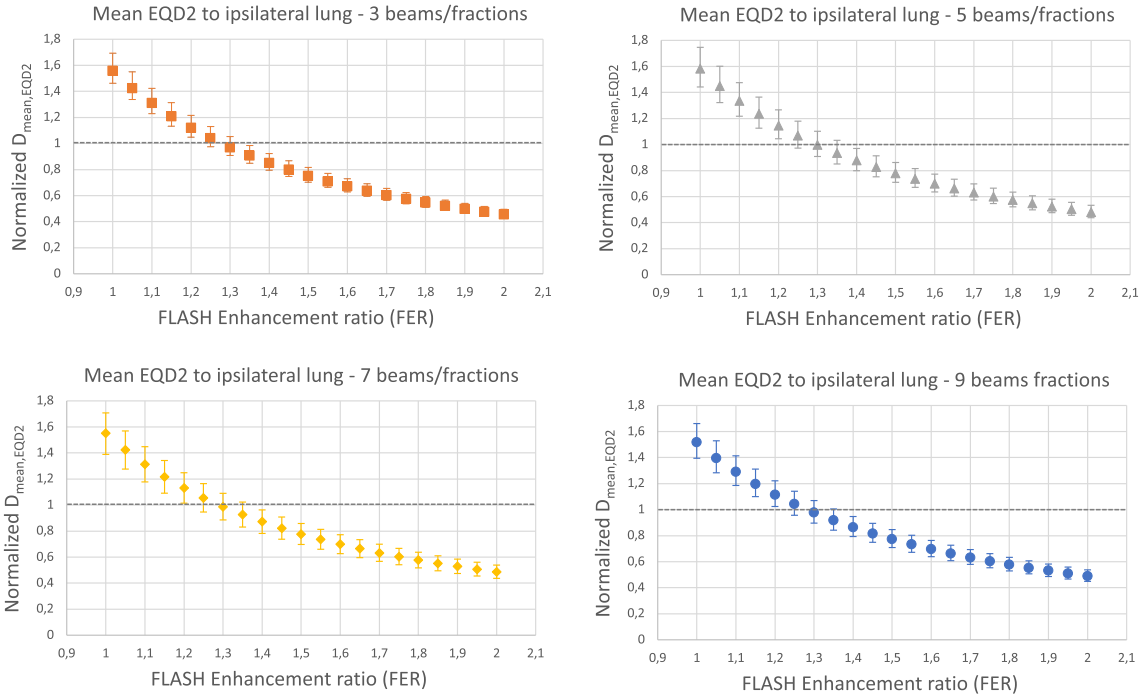

Fig. 3. Dependence on FLASH enhancement ratio (FER) of (a) mean EQD2 to ipsilateral lung and (b) $V_{100\%\ EQD2pres}$ for FLASH enhanced single beam per fraction delivery of SFUD plans with 3 (orange), 5 (gray), 7 (yellow) and 9 (blue) beams/fractions, normalized for each patient to the values attained in conventional ABEF delivery of the same plan. Data points represent the patient population median, error bars indicate the full minimum–maximum population range. Values below 1 indicate the fractionation disadvantage is outweighed by the FLASH effect.

depend on the beam and fraction number and decrease from 1.3 for 3 to 1.1 for 9 beams. FLASH-enhancement has the most impact on plans with a smaller number of beams, where also the $V_{100\%\ EQD2pres}$ without FLASH enhancement is larger (see Table 2). For sufficiently large FERs, the FLASH enhanced dose in all healthy tissue falls below 100% $EQ2D_{pres}$ and the $V_{100\%\ EQD2pres}$ is equal to the GTV.

The panels in Fig. 4 show population break-even FER histograms for $EQD2_{mean}$ and the $V_{100\%\ EQD2pres}$ to the ipsilateral lung. These results confirm that break-even FER for $EQD2_{mean}$ hardly depends on the number of beams and fractions. The transition from FERs for which no patients benefit from FLASH to values for which all patients in this homogeneous group benefit is quite steep, both for $EQD2_{mean}$ and for $V_{100\%\ EQD2pres}$.

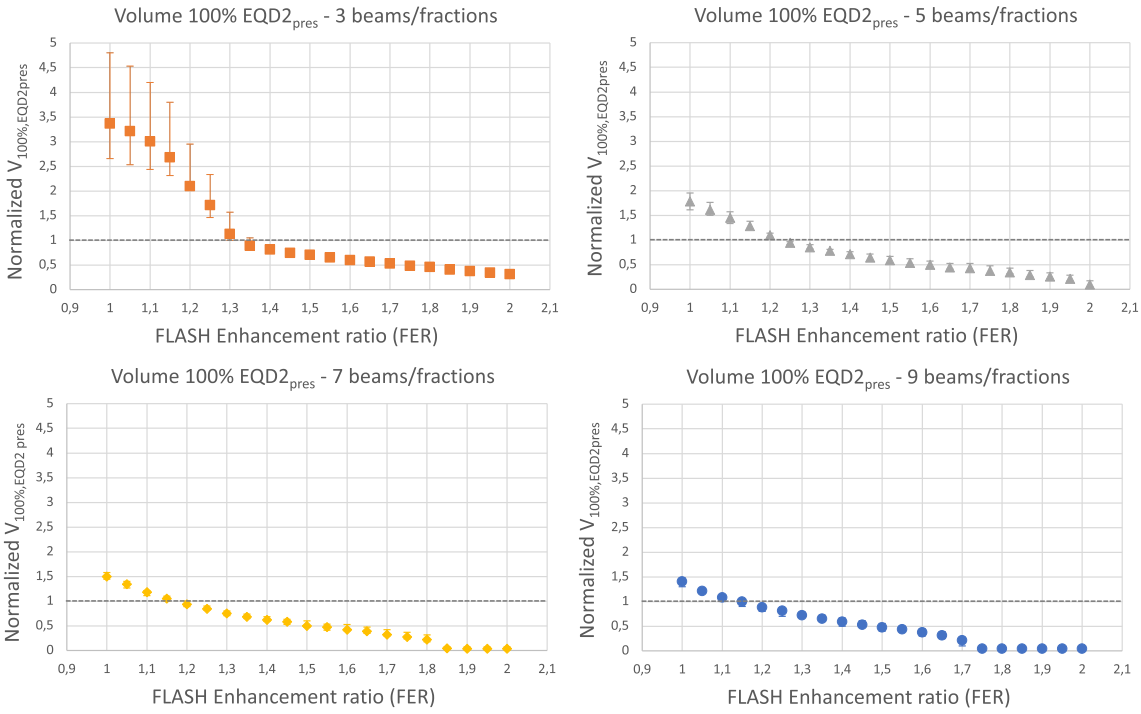

Fig. 3 (*continued*)

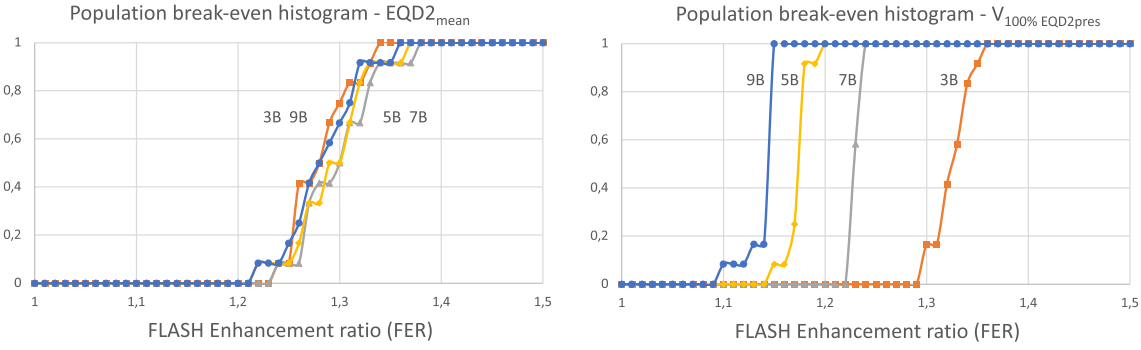

Fig. 4. Population break-even histograms for the $EQD2_{mean}$ to ipsilateral lung and $V_{100\%,EQD2pres}$, i.e., the fraction of patients for which FLASH-enhanced single-beam per fraction delivery is at least at break-even with conventional delivery of all beams in each fraction. Results for plans with 3, 5, 7 and 9 beams/fractions are displayed in orange, gray, yellow, and blue respectively.

Table 3
Number of pencil beam, total beam weight and estimated delivery time per treatment beam.

	Pencil beams per beam	Total beam weight [Gp]	Beam delivery time [ms]	Beam dose rate [Gy/s]
3B	34 (21–99)	170 (130–200)	127 (97–157)	141 (115–185)
5B	33.5 (24–78)	130 (90–230)	99 (73–180)	132 (73–179)
7B	34.5 (24–115)	97 (74–180)	77 (59–144)	136 (73–177)
9B	34 (21–99)	83 (63–190)	67 (51–157)	133 (57–174)

The number of pencil beams per beam, the total beam weights in Gps, the estimated treatment delivery times and the beam dose rates are listed in Table 3. All beam delivery times are below 100 ms. The beam dose rates show a slight decrease with an increasing number of beams and fraction but are all well above the FLASH threshold of 40–100 Gy/s. This confirms that FLASH-compatible delivery of these treatment plans is technologically feasible in principle.

Experimental data on the FLASH effect on lung fibrosis in mice is consistent with a FER larger than 1.8 [1]. This would enable a

population-median healthy tissue sparing of 37%, 30%, 29% and 28% in terms of the $EQD2_{mean}$ and 54%, 66%, 78%, 95% in terms of the $V_{100\%EQD2}$ for plans with 3, 5, 7 and 9 beams respectively.

Discussion

We have investigated the trade-off between fractionation and the FLASH in SBPF delivery of stereotactic treatments for small lung lesions, enabling beam doses above the FLASH dose threshold of about 7 Gy and FLASH-compatible dose rates. Our main finding is that the break-even FER for the mean EQD2 to healthy lung tissue is about 1.3 and hardly depends on the number of beams. For the volume irradiated to 100% of prescribed dose, expressed as an EQD2, we found break-even FERs ranging from 1.3–1.1 for plans with 3 to 9 beams. Since data on lung fibrosis in mice is consistent with a FER larger than 1.8 [1], FLASH enhancement may be within reach in stereotactic proton therapy of lung lesions.

In modeling the FLASH effect, we have made three assumptions: (i) FLASH is a linear local healthy tissue effect, i.e. the FER ratio is applied to non-target voxel doses, (ii) the FER is applied to physical fraction doses and, hence, independent of α/β and (iii) an entire treatment beam is either FLASH or not and FLASH is homogeneous, i.e., possible variations of the FLASH effect within a beam, for instance in the penumbrae, where fraction doses are lower, are neglected. As a result of assumption (i), the trade-off between FLASH and fractionation and, therefore, the break-even point, varies between voxels in a patient. To convert this local variation into of a more global, potentially clinically meaningful dosimetric endpoint, we evaluated the $V_{100\%\ EQD2pres}$ and the $EQD2_{mean}$ to healthy ipsilateral lung. The $V_{100\%\ EQD2pres}$ is quasi-local in that it depends on the small and relatively homogeneous high-dose volume, while the $EQD2_{mean}$ is a more global metric. The $EQD2_{mean}$ depends linearly on dose and volume, as opposed to a near-min/max ($D_{98\%}$/$D_{2\%}$) or an equivalent uniform dose [26] and involves equal weighting of wide range of dose levels. In contrast, the $V_{100\%EQD2}$ is evaluated at one dose level only. Therefore, assumption (i) has limited impact on our results. Based on assumption (ii), the EQD2 was calculated for FLASH-enhanced fraction doses and summed for all fractions. Depending on the FLASH dose threshold, assumption (iii) may be more critical. For a dose threshold of 3.5–7 Gy, the beam doses considered here are well into the FLASH regime, but if it were comparable to the beam dose, higher break-even FERs would have been found [SM]. A better understanding of the dose dependence of the FLASH effect within a beam is essential for its clinical translatability. For a strictly uniform beam doses and fully overlapping beams, the break-even FER increases with dose and with the number of beams [SM].[5] In the clinical treatment plans FLASH may also be attained in voxels where not all beams overlap. Moreover, in optimized treatment plans the break-even FER involves weighted averaging of all voxel doses, including the intermediate and lower (penumbra) doses. This results in lower break-even FERs. Also, as a result of this averaging, the break-even FER for $EQD2_{mean}$ does not significantly depend on the number of beams [SM], as can be seen in Fig. 3a and Fig. 4a.

In modeling fractionation effects, we have assumed a fixed α/β = 3 Gy for all healthy tissue; a lower value would lead to higher break-even FERs and vice versa [SM].[3] We have not considered any possible interference between FLASH and fractionation effects, i.e., a dependence of the α/β on dose rate or dose.

Although a patient's lung function post-treatment depends on dose to both lungs, we focused on dose to the ipsilateral lung as a proxy of healthy tissue damage. The biggest impact of FLASH is expected in the intermediate and high-dose volume surrounding the target. Moreover, dose to contralateral lung may also be reduced by the choice of beam directions. Other dose volume parameters, e.g., $V_{10GyEQD2}$, $V_{15GyEQD2}$ and $V_{20GyEQD2}$ are clinically relevant. But since the corresponding beam dose levels may fall below the FLASH dose threshold when delivered with two or more overlapping beams, these were not included in the analysis presented here.

We have used equiangular arrangements of proton transmission beams maximally avoiding critical serial OARs and minimizing beam overlap in the high-dose volume. Further per-patient fine tuning of beam directions, non-coplanar beams or automated beam selection may be desirable in clinical practice.

Similar considerations and results on FLASH and fractionation may apply to other treatment planning and delivery approaches. In Refs. [17,19], proton transmission beams have been demonstrated to be non-inferior to conventional radiotherapy with photons (VMAT) for stereotactic treatment of small lung lesions. Proton Bragg-peak beams have the disadvantage of increased lateral scattering around the Bragg-peak. Also, placing the Bragg peak in small lung lesions, surrounded by dilute lung tissue, is technologically challenging and comes with substantial range uncertainty. Full IMPT with proton transmission beams may lead to more conformal plans but comes with the challenge of patching fields and a target that moves with respiration between beams and fractions.

The proton energy of 244 MeV used here is the highest energy available in our current beam model. The overall highest dose rate will be achieved at the maximum cyclotron energy of 250 MeV. Although the difference in instantaneous dose rate is substantial, the difference between the lateral profiles and the dose-depth curve in the entrance part of the beam is expected to be small and have little impact on the treatment plans (the Bragg-peak is not inside the patient).

A PTV-based approach was used with transmission beams because the basic assumption underling the PTV-concept in conventional radiotherapy, i.e., the invariance of dose under (small) shifts and deformations, applies to such beams with and SFUD approach, where proton range uncertainty and intensity modulation have been eliminated. The 5 mm GTV-PTV margin used, would be compatible only with state-of-the art breathing motion management, i.e., tracking or gating. Depending on the clinical implementation of stereotactic treatment with proton transmission beams, larger margins, or an internal target volume (ITV) may be needed. This would increase the irradiated volume and, hence, the overall delivery times.

The optimization used here was solely done on physical (beam) dose and dose rates were calculated for each beam as the ratio of the nominal beam doses and estimated delivery times. Depending on the delivery setup used, spot delivery times may fall below the monitor chamber detection times, typically on the order 1–3 ms in which case a lower nozzle current could be used, still leading to FLASH compatible dose rates > 40–100 Gy/s. Alternatively, further pencil-beam reduction [25] may be used in treatment planning. With FLASH models [27] and more advanced FLASH-based dose-rate metrics [28,19] gradually becoming available, a simultaneous optimization of dose rate and dose and/or FLASH-enhanced dose [29], possibly combined with scanning-pattern optimization [30], may become feasible. The question which (dose-rate) metric is most predictive of FLASH in IMPT with PBS is not resolved yet.

[5] In a treatment to 54 Gy in 3 fractions with 3 homogeneous beams, most healthy tissue is irradiated to 3×6 Gy, which, with α/β = 3 Gy, amounts to an EQD2 of 32.4 Gy. With single-beam-per-fraction delivery, most healthy issue is exposed to 1×18 Gy, which corresponds to and EQD2 of 75.6 Gy. If the FLASH effect applies to physical fraction dose, a FER of 1.59 or larger is required to counterbalance this fractionation disadvantage. Similar considerations lead to break-even FERs of 1.82, 1.90 and 1.92 for 65.5 Gy/5, 73.7 Gy/7 and 80.0 Gy/9 treatments. For α/β = 4 Gy, break-even values of 1.56, 2.74, 1.79 and 1.80 are found for regimens with 3, 5, 7 and 9 beams respectively, while α/β = 2 Gy leads to break even at FERs of 1.63, 1.91, 2.04 and 2.09 respectively.

The SBPF approach used here may be extended to treatments with two or more beams per fraction, one above the FLASH dose threshold and one or more below it. In this way an optimal combination of healthy tissue sparing through fractionation and FLASH may be achieved. Overlap between FLASH and non-FLASH beams and the order of irradiation may become important. Further radiobiological research to investigate and optimize such treatments is crucial for the further clinical development of FLASH-PT.

Conclusion

The loss of fractionation in SBPF delivery is substantial, but a FLASH effect outweighing this and resulting in more healthy tissue sparing may be feasible in stereotactic proton therapy of lung lesions. The biggest relative gain in conformity of dose is already achieved with five beams (as compared to three beams), in which case the beam dose of 13.1 Gy is well above the FLASH dose threshold of 7 Gy.

Better understanding of the underlying biology and physiology, and hence of the actual FER, both in radiobiological experiments and in a clinical setting, is crucial for the further development of FLASH radiotherapy. Our results could be used to guide these experiments and serve as a starting point for the design of clinical trials on stereotactic FLASH-PT of small lung lesions.

Conflict of Interest

The department of radiotherapy of the Erasmus MC Cancer Institute received a research grant from the Dutch cancer society and has research collaborations with Elekta AB, Stockholm, Sweden and Accuray Inc., Sunnyvale, USA. HollandPTC has a research collaboration with Varian, Palo Alto, USA.

Acknowledgement

We thank Thyrza Jagt for discussions, Pepík Cruijssen for initial treatment planning, Jasper Kouwenberg for help with commissioning the 244 MeV HollandPTC beam model in Erasmus-iCycle [21] and Marta Rovituso and Kees Spruijt for discussions on delivery parameters.

Appendix A. Supplementary material

Supplementary data to this article can be found online at https://doi.org/10.1016/j.radonc.2022.08.015.

References

[1] Favaudon V, Caplier L, Monceau V, Pouzoulet F, Sayarath M, Fouillade C, et al. Ultrahigh dose-rate FLASH irradiation increases the differential response between normal and tumor tissue in mice. Sci Transl Med 2014;6:245ra.
[2] Bourhis J, Montay-Gruel P, Gonçalves Jorge P, Bailat C, Petit B, Ollivier J, et al. Clinical translation of FLASH radiotherapy: Why and how? Radiother Oncol 2019;139:11–7.
[3] Durante M, Bräuer-Krisch E, Hill M. Faster and safer? FLASH ultra-high dose rate in radiotherapy. Br J Radiol 2018;91:20170628.
[4] MacKay R, Burnet N, Lowe M, Rothwell B, Kirkby N, Kirkby K, et al. FLASH radiotherapy: Considerations for multibeam and hypofractionation dose delivery. Radiother Oncol 2021;164:122–7.
[5] Hornsey S, Alper T. Unexpected Dose-rate Effect in the Killing of Mice by Radiation. Nature 1966;210:212–3.
[6] Montay-Gruel P, Acharya MM, Petersson K, Alikhani L, Yakkala C, Allen BD, et al. Long-term neurocognitive benefits of FLASH radiotherapy driven by reduced reactive oxygen species. Proc Nat Acad Sci 2019;116:10943–51.
[7] Vozenin M-C, De Fornel P, Petersson K, Favaudon V, Jaccard M, Germond J-F, et al. The advantage of Flash radiotherapy confirmed in mini-pig and cat-cancer patients. Clin Cancer Res 2019;25:35–42.
[8] Levy K, Natarajan S, Wang J, et al. Abdominal FLASH irradiation reduces radiation-induced gastrointestinal toxicity for the treatment of ovarian cancer in mice. Sci Rep 2019;10:21600.
[9] Bourhis J, Jeanneret Sozzi W, Gonçalves Jorge P, Gaide O, Bailat C, Duclos F, et al. Treatment of a first patient with FLASH-radiotherapy. Radiother Oncol 2019;139:18–22.
[10] Patriarca A, Fouillade C, Auger M, Martin F, Pouzoulet F, Nauraye C, et al. Experimental Setup for FLASH Proton Irradiation of Small Animals Using a Clinical System. Int J Radiat Oncol Biol Phys 2018;102:619–26.
[11] Smyth LML, Donoghue JF, Ventura JA, Livingstone J, Bailey T, Day LRJ, et al. Comparative toxicity of synchrotron and conventional radiation therapy based on total and partial body irradiation in a murine model. Sci Rep 2018;8:12044.
[12] Zlobinskaya O, Siebenwirth C, Greubel C, Hable V, Hertenberger R, Humble N, et al. The Effects of Ultra-High Dose Rate Proton Irradiation on Growth Delay in the Treatment of Human Tumor Xenografts in Nude Mice. Radiat Res 2014;181:177–83.
[13] Beyreuther E, Brand M, Hans S, Hideghéty K, Karsch L, Leßmann E, et al. Feasibility of proton FLASH effect tested by zebrafish embryo irradiation. Radiother Oncol 2019;139:46–50.
[14] Buonanno M, Grilj V, Brenner DJ. Biological effects in normal cells exposed to FLASH dose rate protons. Radiother Oncol 2019;139:51–5.
[15] Ohsawa D, Hiroyama Y, Kobayashi A, Kusumoto T, Kitamura H, Hojo S, Kodaira S, Konishi T. DNA strand break induction of aqueous plasmid DNA exposed to 30 MeV protons at ultra-high dose rate. J Radiat Res 2021. Epub ahead of print.
[16] FAST-O1 trial, see: https://clinicaltrials.gov/ct2/show/NCT04592887.
[17] Mou B, Beltran CJ, Park SS, Olivier KR, Furutani KM. Feasibility of Proton Transmission-Beam Stereotactic Ablative Radiotherapy versus Photon Stereotactic Ablative Radiotherapy for Lung Tumors: A Dosimetric and Feasibility Study. PLoS ONE 2014;9:e98621.
[18] Van de Water S, Safai S, Schippers JM, Weber DC, Lomax AJ. Towards FLASH proton therapy: the impact of treatment planning and machine characteristics on achievable dose rates. Acta Oncol 2019 Oct;58:1463–9. https://doi.org/10.1080/0284186X.2019.1627416. Epub 2019 Jun 26 PMID: 31241377.
[19] van Marlen P, Dahele M, Folkerts M, Abel E, Slotman BJ, Verbakel WFAR. (2019) Bringing FLASH to the clinic: treatment planning considerations for ultrahigh dose-rate proton beams. Int J Radiat Oncol Biol Phys 2019.
[20] Verhaegen F, Wanders RG, Wolfs C, Eekers D. Considerations for shoot-through FLASH proton therapy. Phys Med Biol 2021;66:06NT01. https://doi.org/10.1088/1361-6560/abe55a. PMID: 33571981.
[21] Heijmen B, Voet P, Fransen D, Penninkhof J, Milder M, Akhiat H, et al. Fully automated, multi-criterial planning for Volumetric Modulated Arc Therapy – An international multi-center validation for prostate cancer. Radiother Oncol 2018;128:343–8.
[22] Kouwenberg J, Penninkhof J, Habraken S, Zindler J, Hoogeman M, Heijmen B. Model based patient pre-selection for intensity-modulated proton therapy (IMPT) using automated treatment planning and machine learning. Radiother Oncol 2021;158.
[23] Kooy HM, Clasie BM, Lu H-M, et al. A Case Study in Proton Pencil-Beam Scanning Delivery. Int J Radiat Oncol Biol Phys 2010;76:624–30.
[24] Timmerman R, Paulus R, Galvin J, Michalski J, Straube W, Bradley J, et al. Stereotactic body radiation therapy for inoperable early stage lung cancer. JAMA 2010;303:1070–6. https://doi.org/10.1001/jama.2010.261. PMID: 20233825; PMCID: PMC2907644.
[25] van de Water S, Kraan AC, Breedveld S, Schillemans W, Teguh DN, Kooy HM, et al. Improved efficiency of multi-criteria IMPT treatment planning using iterative resampling of randomly placed pencil beams. Phys Med Biol 2013;58:6969–83.
[26] Niemierko A. Reporting and analyzing dose distributions: a concept of equivalent uniform dose. Med Phys 1997;24:103–10. https://doi.org/10.1118/1.598063. PMID: 9029544.
[27] Krieger M, van de Water S, Folkerts MM, Mazal A, Fabiano S, Bizzocchi N, et al. A quantitative FLASH effectiveness model to reveal potentials and pitfalls of high dose rate proton therapy. Med Phys. 2022. https://doi.org/10.1002/mp.15459. Epub ahead of print. PMID: 35032035.
[28] Folkerts MM, Abel E, Busold S, Perez JR, Krishnamurthi V, Ling CC. A framework for defining FLASH dose rate for pencil beam scanning. Med Phys 2020;47:6396–404. https://doi.org/10.1002/mp.14456. Epub 2020 Nov 15. PMID: 32910460; PMCID: PMC7894358.
[29] Gao H, Lin B, Lin Y, Fu S, Langen K, Liu T, et al. Simultaneous dose and dose rate optimization (SDDRO) for FLASH proton therapy. Med Phys 2020 Dec;47:6388–95. https://doi.org/10.1002/mp.14531. Epub 2020 Nov 8 PMID: 33068294.
[30] Kang JH, Wilkens JJ, Oelfke U. Demonstration of scan path optimization in proton therapy. Med Phys 2007;34:3457–64. https://doi.org/10.1118/1.2760025. PMID: 17926947.